RSC Applied Polymers

Accepted Manuscript

This article can be cited before page numbers have been issued, to do this please use: A. Caridi, A. Kurowska, E. Lizundia and J. Worch, *RSC Appl. Polym.*, 2026, DOI: 10.1039/D5LP00403A.

ROYAL SOCIETY OF CHEMISTRY

rsc.li/RSCApplPolym

View Article Online
DOI: 10.1039/D5LP00403A

Tunable Enhancement of Polyester Biocomposites Via Extrusion with Fungi-derived Chitin

Authors: Adam T. Caridi,[1,2] Amelia Kurowska,[1,2] Erlantz Lizundia,[3,4*] Joshua C. Worch[1,2*]

Affiliations:

[1]Department of Chemistry, Macromolecules Innovation Institute, Virginia Tech, Blacksburg, VA, USA

[2]Macromolecules Innovation Institute, Virginia Tech, Blacksburg, VA, USA

[3]Life Cycle Thinking Group, Department of Graphic Design and Engineering Projects, Faculty of Engineering in Bilbao, University of Basque County (EHU), Bilbao 48013 Spain

[4]BCMaterials, Basque Center for Materials, Applications and Nanostructures, UPV/EHU Science Park, 48940 Leioa, Spain.

*Corresponding authors. Email: erlantz.liizundia@ehu.eus or jworch@vt.edu

Abstract:

Chitin is a polysaccharide that serves as a useful filler component to blend with conventional plastics and afford melt-compounded biocomposites with tunable properties. However, chitin is typically isolated under harsh conditions from crustacean exoskeletons, limiting large-scale production and jeopardizing its environmental sustainability. Agricultural sources, such as fungi, offer a more sustainable and reliable feedstock for the upscaled production of chitin. Yet, the use of chitin obtained from these feedstocks remains underexplored as a filler component in melt-compounding applications. Herein, we describe the first use of fungi-derived chitin nanofibrils, which are harvested from commercially cultivated mushrooms, as a melt-compounding additive for polyester-based biocomposites synthesized using twin-screw extrusion. A Design of Experiments approach surveyed extrusion parameters such as screw speed, mixing time, and filler loading to develop structure-processing-property relationships. The fungi-derived chitin nanofibril biocomposites generally feature enhanced stiffness compared to benchmark materials incorporating commercially sourced shrimp shell-derived chitin. Interestingly, the fungi-based materials also display enhanced alkaline degradability as compared to the benchmark biocomposites, opening the door towards the design of mechanically functional yet easily degradable materials that could be useful in sustainable packaging applications. This study shows that fungi, which are widely cultivated under controlled conditions, yield a viable source of chitin that can be used as a competitive filler in polyester biocomposites.

View Article Online
DOI: 10.1039/D5LP00403A

Polyesters are important polymers used across many commercial settings, including textiles, packaging, films, and biomedical applications.[1-3] Aliphatic polyesters such as polylactic acid (PLA), poly3-hydroxyalkanoates (PHAs), and polycaprolactone (PCL) generally feature enhanced biocompatibility and degradability compared to conventional aromatic polyesters such as polyethylene terephthalate (PET).[1-4] However, aliphatic polyesters have yet to emerge as a mainstream single-use plastic product as they often do not possess the requisite mechanical and thermal properties compared to aliphatic counterparts such as polyolefins,[5] or aromatic polyesters such as PET. To improve the mechanical and thermal integrity of PCL and other aliphatic polyesters, fillers are typically added to reinforce the polymer matrix and create composites.[6] It is desirable for the filler to be renewably sourced and possess high biocompatibility and biodegradability while also being inexpensive, especially when these composites are used in packaging or agricultural applications.[7] The development of sustainable materials emphasizes the use of raw materials and the avoidance of potential adverse effects arising from their disposal as waste. As such, biobased materials including cellulose nanocrystals (CNCs), starch, lignin, chitosan, and chitin, among others have been investigated as filler components alongside polyester matrices.[8-13]

Among polysaccharides, chitin is the second-most abundant feedstock with applications across many areas such as sensing, drug delivery, packaging, tissue engineering, and optics.[14-17] Although cellulose is a more abundant biopolymer than chitin, it typically must be extracted from lignocellulosic biomass which involves many process-intensive steps that typically yield large amounts of intractable lignin-rich tars.[18, 19] In comparison, chitin extraction byproducts (protein-rich solids, calcium carbonate, lipids, and pigments) can be readily handled.[20] However, chitin's suitability for valorization depends on feedstock-specific chitin content, purity, and mostly, its isolation conditions.[17] Crustacean shells, such as those derived from shrimp, are now the primary feedstock for commercial chitin, which is a precursor for chitin nanocrystals (ChNCs). However, isolation of the latter from commercial chitin (which itself underwent intensive extraction steps from the biological source) requires treatment with concentrated acid (~3 M HCl) at temperatures above 90°C with overnight reactions to remove native inorganic matter.[21]

In this context, other chitin sources are currently being investigated in an endeavor to employ milder isolation processes. Fungi, or mushrooms, are an attractive feedstock for chitin production since they grow quickly and can be cultivated across diverse environments. Moreover, harvesting chitin from mushrooms directly yields chitin nanofibrils from an efficient extraction process that produces little waste (alkaline wash of dried mushrooms at 65 °C, 3 h), although this process is not yet industrialized.[22] Due to these efficiency gains, chitin sourced from mushrooms offers a lower environmental footprint according to life cycle assessment (LCA) when compared to established supply chains from crustacean-derived chitins.[15]

To date, chitin has been widely used as a low-volume filler (typically ≤ 5 wt%) to modulate the mechanical properties of polyester biocomposites with twin screw extrusion (TSE) being the most industrially applicable method for production.[23-25] However, optimization of processing conditions for TSE melt-compounding are rarely reported.[26] This is a critical gap as processing parameters such as mixing time, screw speed, and temperature may have a substantial effect on final properties of the biocomposite.[27, 28] Moreover, all prior examples of melt-compounded polyester-chitin biocomposites employed shrimp-shell derived commercial chitin (SC), whereas this is the first report of using fungi-derived chitin nanofibrils (ChNFs) as a filler for melt-compounding. While there are a few examples of biocomposites developed from ChNFs, these studies employed non-scalable solvent-casting techniques.[29] Thus, it is unknown if

View Article Online
DOI: 10.1039/D5LP00403A

mushroom-derived chitin can serve as a viable drop-in replacement for existing crustacean-derived chitin sources in melt-compounding formulations, as other biomolecules (such as pigments or proteins) may be present in the former.

Herein, we investigate TSE melt-compounding of PCL and mushroom-derived ChNFs to afford biocomposites with up to 20 wt% chitin which were compared to biocomposites from commercial SC (used as received without further processing) as a benchmark. This work demonstrates an uncommon case in which TSE parameters were systematically surveyed by a design of experiments (DoE) following a Box-Behnken design (BBD) model to study the effects of processing conditions and chitin loading on thermomechanical properties of the biocomposite. Materials formed from mushroom-derived ChNFs display enhanced stiffness and more rapid hydrolytic degradation of the PCL matrix compared to samples synthesized using shrimp-shell derived chitin. We attributed these effects to unique morphological differences that have downstream impacts on their physical characteristics. These findings suggest that agricultural products are a viable source of high-quality chitin that can be used to manufacture biocomposites with tunable physicochemical and thermomechanical properties.

RESULTS & DISCUSSION

The chitin (isolated as ChNFs) used in this work was sourced from *Agaricus Bisporus*, a common food-grade mushroom, and stored in a 2.5 wt% aqueous dispersion after alkaline extraction according to a prior report (**Fig. 1a**).[30] The ChNFs were then reclaimed from the aqueous dispersion via freeze drying and subsequently pulverized into a powder via grinding that was suitable for the extrusion processes. Our pulverization process was not finely controlled but prior reports suggest that smaller particle sizes may lead to more homogeneous composites at shorter mixing times.[31] The extruded biocomposites were then hot-pressed into thin films suitable for thermomechanical testing.

View Article Online
DOI: 10.1039/D5LP00403A

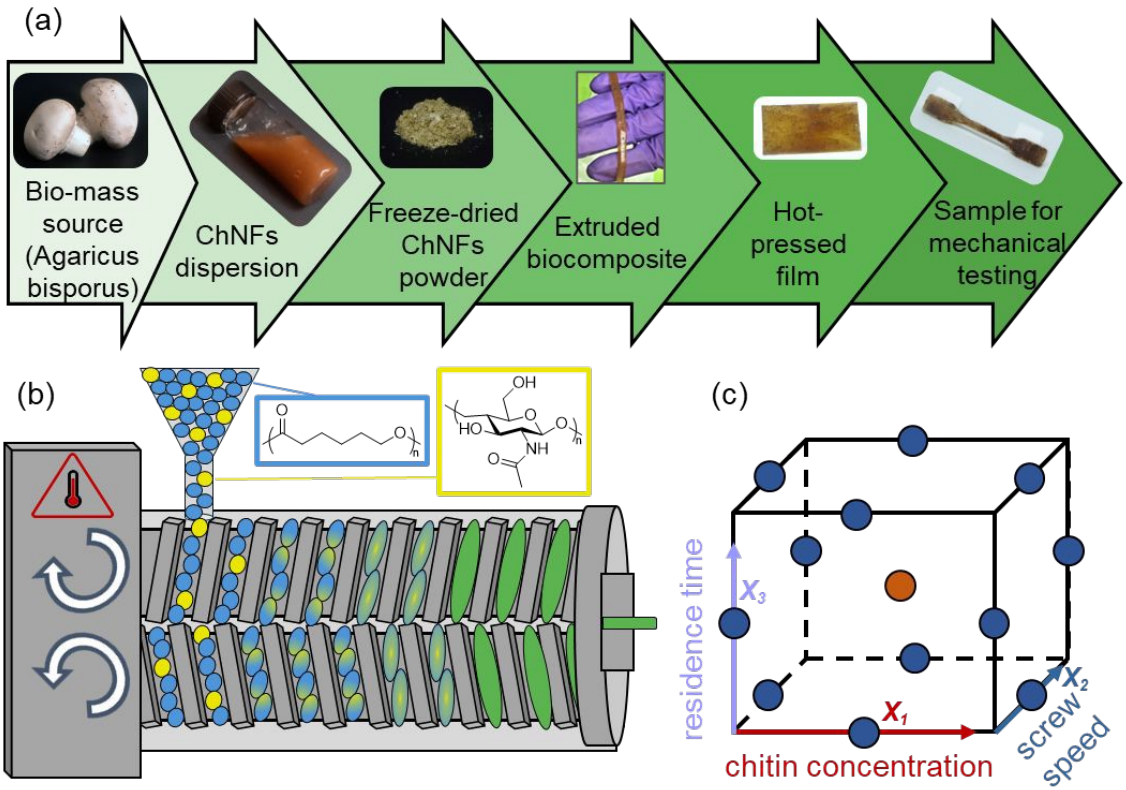

Figure 1. Synthesis of PCL/ChNFs biocomposites (a) Overview of ChNFs extraction and processing to afford the biocomposite films, (b) cartoon schematic of twin screw extrusion process for biocomposite manufacture, (c) Box Behnken design model used to optimize material properties via three extrusion parameters.

During extrusion, PCL and chitin were simultaneously added to ensure uniform melt compounding; we also employed an extruder configuration with counter-rotating screws instead of co-rotating screws to avoid a high shear environment, the latter of which promoted the formation of bubbles and heterogeneities in the composite during early trials (**Fig. 1b**).[32] Extrusion parameters were surveyed with a DoE study following a three-factor BBD, which operates on a response surface methodology to optimize a process with multiple variables (**Fig. 1c**).[33] For the DoE screening, commercial SC was employed as a model filler to blend with PCL (affording PCL_{SC}) due to the large quantity of chitin needed to complete all extrusion experiments and for future comparison to ChNFs-based biocomposites (PCL_{ChNFs}, vide infra); the commercial SC was not processed further in our hands before use and is expected to possess differences in morphology and thermal properties compared to ChNFs.[16, 34] Thus, the DoE responsive tunability observed from the PCL_{SC} biocomposite may not translate identically. However, it will afford a baseline benchmark for comparison to the ChNFs biocomposites. Furthermore, we selected a BBD instead of a central composite design (CCD) since the former is considered more efficient, i.e., smaller experimental burden by not requiring factorial corner points and affords a second-order model. When determining the bounds of a BBD, the max and min values inputed are the actual max and min, in contrast to that of a CCD, which entails a full factorial cube and axial points, which dramatically increases the number of required experiments. Further, a BBD exhibits second-order models because the edge-midpoint and center-point structure provide all the information needed to estimate linear, interaction, and quadratic terms. In other words, the geometry of the design

View Article Online
DOI: 10.1039/D5LP00403A

inherently captures curvature without requiring extreme corner points. Three independent variables were explored, with lower and upper bounds and a middle point: chitin concentration (5-20 wt%), mixing speed (25-200 rpm), and mixing time (45-180 s). This parameter range was selected to cover the conventional extrusion conditions encountered in polymer processing. The temperature was fixed at 100 °C as we determined that this temperature yielded minimal torque during extrusion without inducing thermal degradation of the polymer matrix. Additionally, a 180-second pre-mix step was applied to all experiments as the initial introduction of PCL and chitin into the screws causes a high torque associated to the melting and transport of the material throughout the screws. The output of these parameters afforded a permutated run order with 12 unique conditions plus five central-point repeats (17 unique conditions in total) to mitigate machine processing fluctuation. To ensure accuracy of the model (**Table S4)** all DoE trials were completed within a two-day period and the extruded biocomposites were stored in a desiccator to mitigate environmental factors before further processing.

The extruded samples were then hot-pressed into films (100 °C, 15 min) for thermomechanical analysis; each film was also stored in a desiccator and tested within 24 h to minimize aging effects on the material. Each unique sample from the DoE trial was analyzed via thermogravimetric analysis (TGA), dynamic mechanical thermal analysis (DMTA), and uniaxial tensile testing (**Table S4**). This information was used to select five representative conditions for PCL_{SC} biocomposites. Analogous samples where ChNFs were substituted for SC were prepared to afford PCL_{ChNFs} biocomposites (**Table S5**). Fourier transform Infrared (FTIR) and Raman spectroscopy were used to confirm incorporation of chitin throughout the composites. FTIR spectroscopy of the biocomposites show that amide C=O stretches (~1623; 1655 cm^{-1}) from chitin are poorly resolved from the PCL ester C=O stretch, however the chitin band near (~1550 cm^{-1}) due to amide N-H bending and C-N stretching is apparent (**Fig. S2**). Additionally, FTIR spectroscopy of the neat chitin samples were performed. ChNFs are characterized by typical chitin absorption features, including a broad band at 3650–3200 cm^{-1} due to –OH stretching; –CH bands at 2911 and 2841 cm^{-1}; amide I, II and III bands at 1628, 1556 and 1315 cm^{-1}, respectively; and sharp peaks at 1378 and 1029 cm^{-1} due to CH3 symmetrical deformation and C–O–C groups in chitin, respectively.[35, 36] The presence of the amide III band confirms that the alkaline treatment applied during top-down isolation is mild enough to maintain the structure of chitin and avoid its conversion into chitosan. The fact that the amide bands are less resolved compared to the SC sample is ascribed to the presence of covalently bound β-glucans.[22] We then determined the degree of acetalization (DA) by using the amide I band at 1655 cm^{-1} as a measure of the N-acetyl group content and comparing this to the hydroxyl group at 3430cm^{-1}, which acts as an internal standard (**Fig. S3 and Eq. 3**).[37-39] Both samples showed high DA (SC = 94.5%; ChNFs = 93.5%). For Raman spectroscopy, the biocomposites displayed strong Raman signals between 1100-1650 cm^{-1}, which is indicative of chitin in the sample, whereas PCL is Raman inactive in the same region (**Fig. S3-5**); these profiles were spatially consistent across different regions of the sample, which suggests a uniform incorporation.

View Article Online
DOI: 10.1039/D5LP00403A

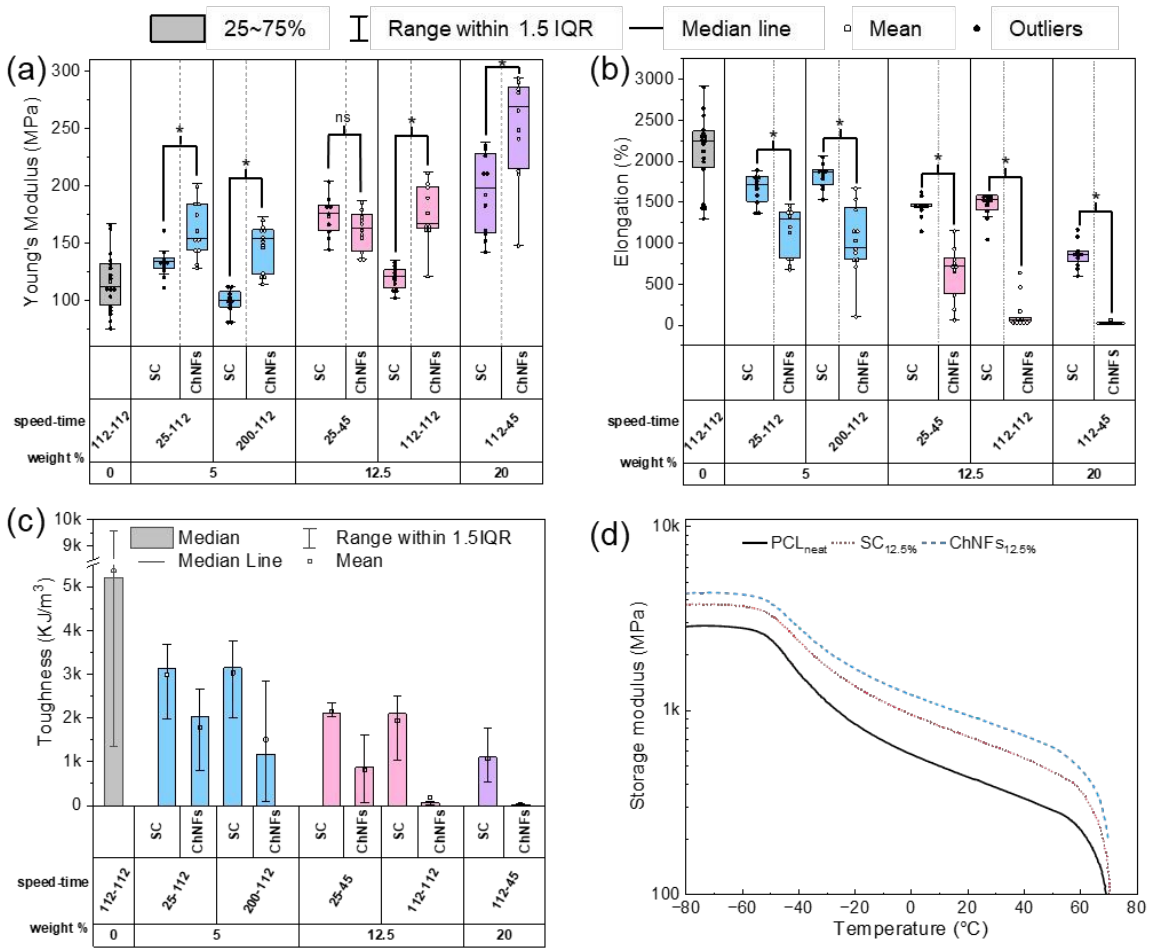

Figure 2. Mechanical properties data for PCL/chitin biocomposites correlated to processing parameters and composition. (a) Young's modulus (n = 9), (b) Elongation at break (n = 9), (c) Tensile toughness (n = 9), (d) Representative thermograms from DMTA temperature sweeps (−80 to 80 °C, 1 Hz, 1% strain, n = 9). Statistical analysis was performed using an ordinary two-way ANOVA test ($p < 0.05$). Error bars represent 1 s.d.

Mechanical testing of the materials via uniaxial tensile analysis showed that the biocomposite samples were generally more rigid and less ductile and revealed unexpected effects of process parameters (**Fig. 2, Fig. S17-32**). We anticipated some distinction here between SC and ChNFs biocomposites since chitin morphology and crystallinity are typically dependent on feedstock source and specific processing conditions.[34] The Young's modulus was positively correlated with chitin content in PCL_{ChNFs} reaching a maximum value for the samples with 20 wt% ChNFs (**Fig. 2a**). This enhanced stiffness is expected as the ChNFs have a higher modulus than PCL.[29] Yet, the trend was less clear in PCL_{SC} where several samples (5 wt% and 12.5 wt% chitin) possessed a relatively lower stiffness to PCL_{ChNFs}. All conditions except the middle condition (12.5%-25rpm-45sec) were statistically different ($p < 0.05$) between the chitin types (**Fig. 2a; Table S8**). Interestingly, the screw speed was also impactful to PCL_{SC} samples where more rapid mixing generally led to lower modulus values, although this was not observed for PCL_{ChNF}. The yield strength slightly decreased with the incorporation of more fillers and a large decrease in UTS was observed due to an overall decrease in ductility which limited strain-hardening as compared to PCL (**Fig. S17-21**). However,

View Article Online
DOI: 10.1039/D5LP00403A

the PCL_{SC} samples consistently displayed greater ductility than PCL_{ChNFs} counterparts at all conditions to a statistically significant degree ($p = 0.05$) (**Fig. 2b; Table S9**); this is congruent with their relative differences in stiffness and was most pronounced for the 20 wt% formulations. Nevertheless, the PCL_{ChNFs} materials were not brittle and showed plastic deformation for all formulations (**Fig. S28-32**). The superior ductility for PCL_{SC} generally led to higher toughness values although a comparison of the 5 wt% samples showed that there was no statistical difference between the two (**Fig. 2c**). Their overall mechanical performance, even for the 20 wt% samples, compares favorably against some thermoplastic starch samples used in flexible packaging applications (e.g. UTS = 4.7-9.8 MPa; Young's modulus = 120-160 MPa; elongation at break ≈ 50%).[40, 41] Flexible packaging plastics require adequate tensile strength and stiffness paired with the ability to undergo plastic deformation under high stresses (typically UTS > 10 MPa; Young's modulus > 100 MPa; elongation at break > 20%) alongside good gas and moisture barrier properties.[42] The mechanical performance of our biocomposites is suitable for flexible packaging although their barrier properties are not yet known. Our biocomposites are generally more ductile than PLA but less strong and stiff (PLA UTS = 50-70 MPa; Young's modulus > 1 GPa), however PLA is inherently brittle (elongation at break < 10%) and must be plasticized to be made flexible. Another emerging bioplastic for packaging is polybutylene succinate (PBS) which is weaker and less stiff than PLA (UTS = 30-35 MPa; Young's modulus = 300-500 MPa) but it is more ductile (elongation at break >100%) and commonly blended with other bioplastics such as PLA.[43]

DMTA thermograms corroborated tensile data where both biocomposites possessed a glassy and rubbery modulus compared to PCL, and PCL_{ChNFs} had superior values relative to PCL_{SC}. Together, these results confirm the reinforcing role of the polysaccharide within the biocomposite. The glass transition temperature (tanδ ≈ −30 °C) and flow temperature (≈ 65 °C) were similar across all tested samples which suggests that the chitin filler did not disrupt the thermal properties of the PCL matrix (**Fig. 2d; Fig. S33-37**).

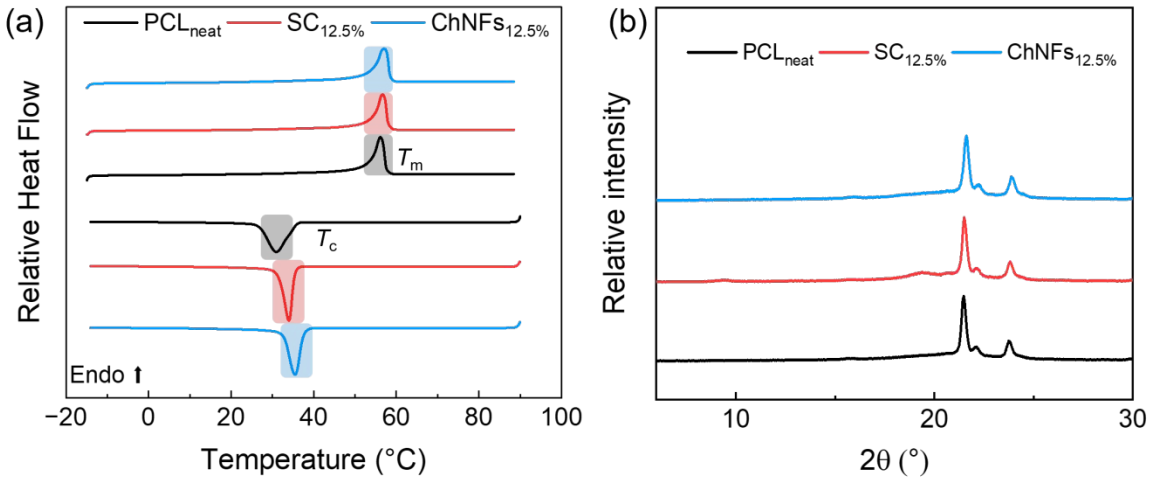

Figure 3. Thermal properties of 12.5% PCL/chitin biocomposites. (a) DSC thermograms depicting T_m and T_c (b) XRD patterns of thin films.

Differential scanning calorimetry (DSC) heating cycles showed that the T_m and percent crystallinity are relatively unaffected by filler loading (**Fig. 3a; Fig. S13-16; Table S7**). This may seem counterintuitive since particles may increase the crystallinity of composites however this enhancement is usually dependent

View Article Online
DOI: 10.1039/D5LP00403A

on both particle size and shape which often have ambiguous structure-property relationships.[44, 45] On the other hand, the crystallization kinetics are accelerated as evidenced by slightly higher T_c values; this is possibly due to ChNFs acting as nucleation sites.[46] XRD patterns of the PCL_{ChNFs} biocomposites demonstrate the incorporation of chitin does not alter the crystalline morphology of the bulk sample (**Fig. 3b, Fig. S37**). The diffraction pattern of PCL (two sharp diffraction peaks centered at 2θ = 21.5° and 23.8°)[47, 48] is not modified by the incorporation of chitin, except for the presence of a minor peak located at approximately 2θ = 19.7°. This minor signal increases in intensity with the presence of chitin and is consistent with the *(110)* reflection of α-chitin, which organizes into a two-chain orthorhombic unit cell.[49, 50] Neat XRD spectra were obtained for both SC and ChNFs (**Fig. S40**). The XRD pattern of ChNFs is characteristic of a semi-crystalline polymeric material (diffraction peaks over an amorphous halo), with two broad crystalline peaks centered at 2θ = 9.2 and 19.7º, which could be identified with the (020) and (110) planes of α-chitin.[35] The SC spectrum exhibited sharper peaks that align with the planes of α-chitin. The presence of β-glucans that cannot be completely removed during alkaline isolation likely gives the material a comparatively more amorphous character.[22] Furthermore, these differences in diffraction patterns may also be explained by the intrinsic differences in chitin crystallinity, which is source dependent; crustacean-derived chitin is typically possesses a higher degree of crystallinity than chitin obtained from fungal sources.[16]

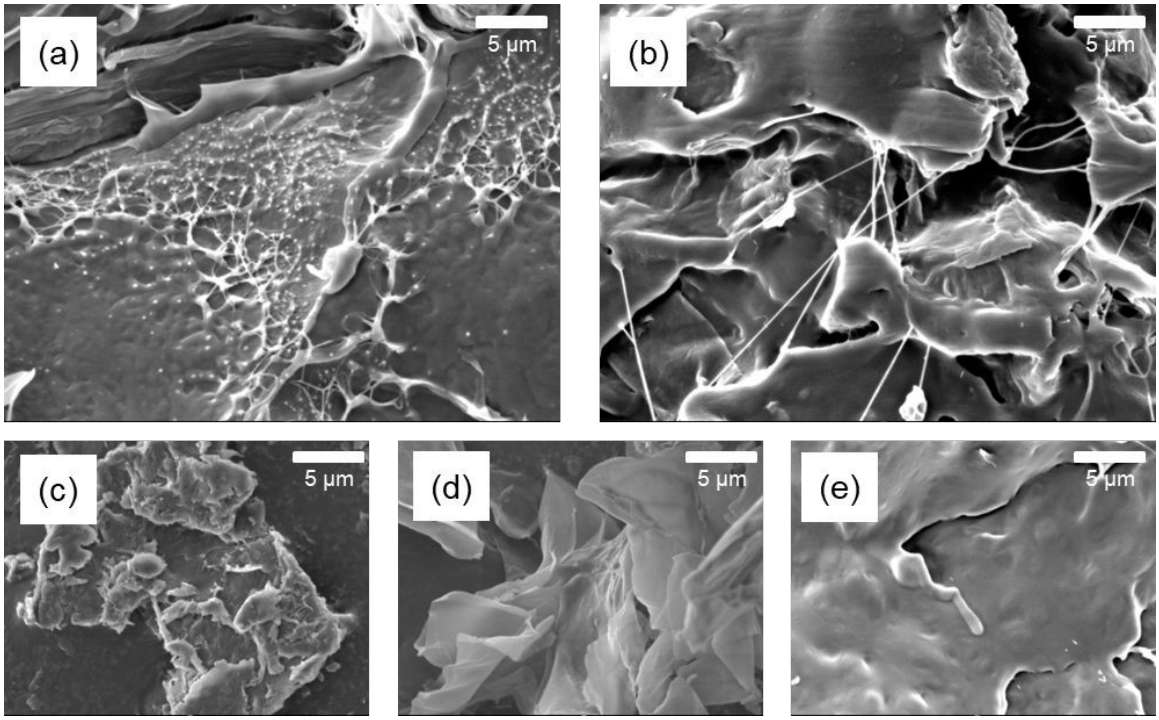

Figure 4. SEM micrographs of PCL/chitin biocomposites and their constituent materials. (a) PCL_{SC}, (b) PCL_{ChNFs}, (c) SC_{neat}, (d) $ChNFs_{neat}$, (e) PCL_{neat}.

We then studied the morphology of the SC- and ChNFs-based biocomposites using scanning electron microscopy (SEM) to elucidate the distinct differences in mechanical properties between the two materials (**Fig. 4**). The samples were prepared by cryogenic fracturing, where the surface was pre-scored and cooled to cryogenic temperatures (−196 °C) before fracture and then adhered to a 90-degree mount and sputter-coated. The PCL_{SC} biocomposite shows chitin aggregation consistent with the immiscibility of the two

View Article Online
DOI: 10.1039/D5LP00403A

components (**Fig. 4a**); this feature was spatially consistent throughout the sample. In contrast, the PCL_{ChNFs} biocomposite showed fibrous strands that presumably serve as reinforcing agents to stiffen the bulk material (**Fig. 4b**). This nanofiber bridging may be responsible for the enhanced Young's modulus observed for the PCL reinforced with fungi chitin. Moreover, these fibers are attached at multiple "anchor points" throughout this cross-sectional area and are assumed less taut when the composite is not fractured. These morphological differences showing greater distribution and coverage of the fibrous ChNFs filler may also explain differences in degradation temperatures ($T_{d5\%}$) as it decreased as chitin content increased, and this was especially pronounced for ChNFs samples going from 374°C for PCL_{neat} to 328°C and 266°C for SC and ChNFs, respectively (**Fig. S7-S12; Table S6**). The constituent materials were also assessed using SEM with SC_{neat} showing micron-sized agglomerates, which are presumably fractured and homogenized throughout the biocomposite during the extrusion process (**Fig. 4c**). In comparison, $ChNFs_{neat}$ has a distinct morphology as it does not form well-defined agglomerates in its native state (**Fig. 4d**). Finally, the PCL samples possessed a sheet-like lamellar morphology from fractured spherulites which is consistent with semicrystalline polymers (**Fig. 4e**).[51]

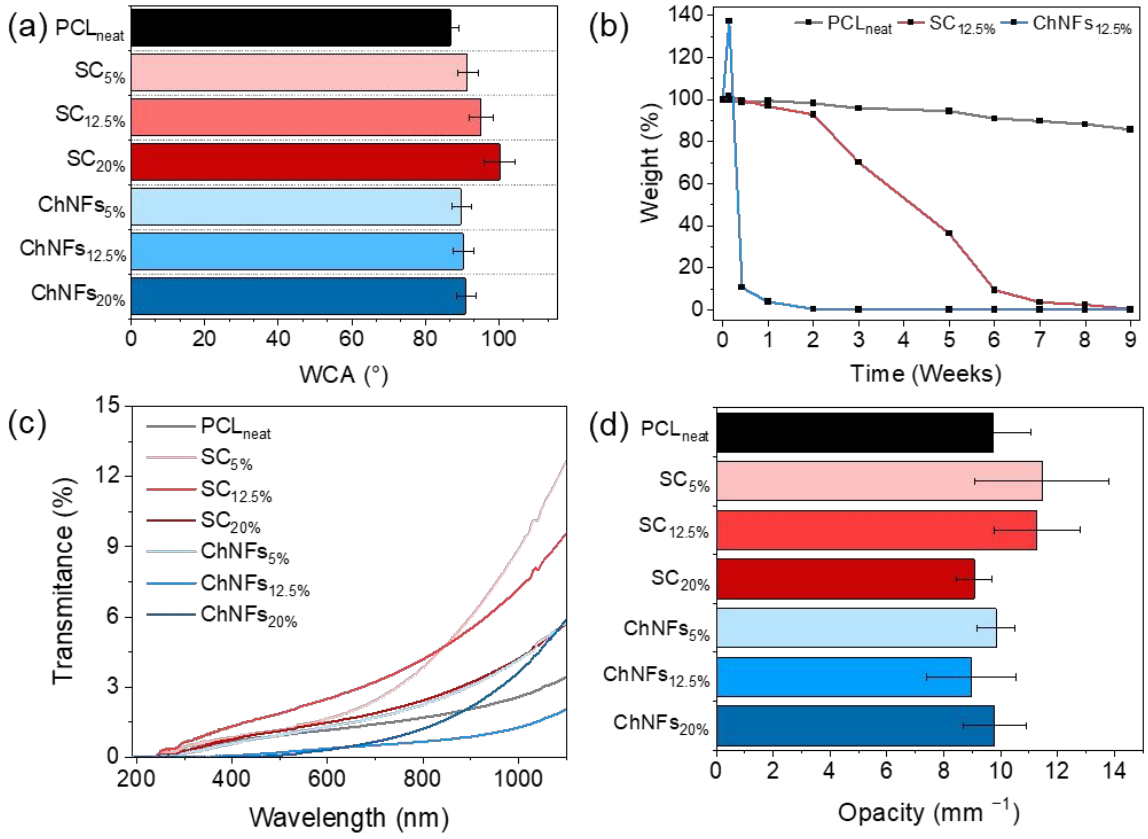

Figure 5. Physicochemical and optical properties of PCL/chitin biocomposites compared against PCL control sample: (a) Water contact angle values for water drops on the surface of thin films; (b) Hydrolytic degradation of thin films in 1M NaOH; (c) UV-Vis transmittance spectroscopy; and (d) resulting opacity values for thin films (λ = 600 nm). Error bars represent 1 s.d.

View Article Online
DOI: 10.1039/D5LP00403A

Surface wettability is an important parameter for end-use applications of plastic materials and this was assessed using static water contact angle (WCA) experiments.[52] The PCL film displays a hydrophobic nature as revealed by the WCA value of 86.9 ± 2.1°. The addition of both SC and ChNFs increases the surface hydrophobicity of the film to maximum WCA values of 100.3 ± 4.3° and 91.0 ± 2.7°, respectively (**Fig. 5a, Fig. S41**). These results may seem counterintuitive given chitin's comparatively high affinity for water, however there are several additional factors to consider. ChNFs are composed of a glucan-chitin complex, which have a relatively lower polarity due to the incorporation of hydrophobic proteins such as the cysteine-rich hydrophobins.[34] Furthermore, the incorporation of chitin may introduce micro- or nanoscale roughness, effectively increasing the bulk hydrophobicity via the Cassie-Baxter effect.[53]

We also examined the hydrolytic degradation of the PCL/chitin biocomposites alongside PCL as a control (**Fig. 5b, Fig. S42-47**). PCL shows relatively good hydrolytic stability, matching prior literature.[54] Both biocomposites displayed enhanced degradability compared to non-reinforced PCL, especially under accelerated alkaline conditions,[55] despite their relatively greater hydrophobicity. This feature could be exploited in post-consumer waste treatment facilities (e.g. alkaline hydrolysis under controlled conditions) and it would be expected to increase the relative environmental degradation of the biocomposites compared to PCL if released into the environment. The biocomposites also showed greater bulk swelling compared to PCL which is likely a key factor for their faster degradation rates. Here, degradation refers to fragmentation of the sample that leads to dispersing of chitin particles and PCL particles in the medium. Although we did not track the fate of the released particles, the PCL particles would be expected to subsequently hydrolyze more rapidly than a cohesive film due to their increased surface area.[56] Furthermore, there were surprising differences between PCL_{SC} and PCL_{ChNFs}. In fact, PCL_{ChNFs} degraded significantly faster (~5 fold) than its PCL_{SC} counterpart, where bulk degradation of the former was observed within approximately 7 days under alkaline conditions. The stark differences in degradation behavior between the two chitin materials can be attributed to distinct swelling behaviors within the first 24 h of submersion in the solution. The PCL_{ChNFs} sample swelled > 4-fold faster compared to PCL_{SC} and reached 147% of its initial mass (overall water uptake), before onset of bulk degradation, compared to a value of < 105% for PCL_{SC} (Fig. S48-53). This was remarkable considering the two PCL/chitin samples had identical compositions and processing parameters. This enhanced water uptake may be explained by the lower intrinsic crystallinity of the fungi-derived chitin (which coexists with amorphous β-glucans) since the DA is similar for both chitin samples.[28] Although little degradation was observed under neutral conditions (PBS buffer) within our experimental timeframe, substituting PCL with polyesters that display superior biodegradability, such as poly(butylene succinate) PBS or poly(hydroxy alkanoates) PHAs,[57] would be expected to enhance degradation rates under more benign conditions.

Moreover, colorimetric analyses reveal the color differences when chitin is added to neat PCL film; these parameters include lightness difference (ΔL*), chroma difference (ΔC*) and overall color difference (ΔE*) relative to the neat PCL film (**Table S10**). ΔE* significantly increases with chitin concentration to a maximum of 49.4 ± 8.3 at 20 wt% ChNFs. Similarly, ΔL* (indicating darkening) and ΔC* (indicating brighter color) change more significantly with the addition of ChNFs in comparison to samples containing shrimp shell chitin. These results indicate that the original color profile of PCL is better preserved in the presence of shrimp shell chitin as compared to the fungi chitin extract; this could be due to the presence of chromophores (e.g. pigments) in the latter. Finally, the optical properties of the composite films were assessed by transmittance mode ultraviolet-visible (UV-Vis) spectroscopy. All the films are characterized

View Article Online
DOI: 10.1039/D5LP00403A

by a low optical transmittance in the UV and visible regions (λ = 190-800 nm) which is not unexpected given their crystalline nature (**Fig. 5c**). The film opacity of the neat PCL film at λ = 600 nm (the midpoint of the visible range)[58] is around 9.5 mm^{-1} and no clear trend is observed from the addition of chitin (**Fig. 5d**).

CONCLUSION

In summary, mushroom-derived chitin was assessed alongside traditional crustacean-based chitin feedstocks in melt-compounding extrusion applications to afford biocomposites with up to 20 wt% chitin incorporation. We demonstrated the tunability of properties (such as mechanical and degradation) based on a detailed study of extrusion parameters via a Box-Behnken DoE, which is not commonly reported in the literature for biocomposite formulations. The mushroom-based biocomposites showed enhanced stiffness and accelerated degradation rates in aqueous alkaline media as compared to analogous materials incorporating crustacean-derived chitin. This study shows that fungi yield a viable source of chitin which can be used as a drop-in replacement filler for PCL-based composites. Importantly, we anticipate this approach to be applicable for other aliphatic polyester matrices such as PBS and PHAs, which are widely employed for packaging and agricultural films.[7] Finally, chitin is an inexpensive filler and the high loading content (up to 20 wt%) could make these and related biocomposites more economical.

ACKNOWLEDGEMENTS

Funding: JCW acknowledges start-up funding from Virginia Tech. EL acknowledges funding from the University of the Basque Country (EHU) through the "Convocatoria de ayudas a grupos de investigación" GIU21/010 grant. This work was made possible by the use of Virginia Tech's Tiedemann Materials Characterization Facility, which is supported by the Institute for Critical Technology and Applied Science (ICTAS), the Macromolecules Innovation Institute (MII), and the Office of the Vice President for Research and Innovation.

Author contributions: JCW and EL conceived the work and directed the research. JCW, ATC, and EL designed the experiments. ATC, EL, and AK performed and analyzed experiments. JCW and ATC prepared the manuscript, and all authors contributed to manuscript revisions.

Competing interests: None

Data and materials availability: All data are available in the manuscript or the supplementary information.

REFERENCES

1. A. Chamas, H. Moon, J. Zheng, Y. Qiu, T. Tabassum, J. H. Jang, M. Abu-Omar, S. L. Scott and S. Suh, *ACS Sustain. Chem. Eng.*, 2020, **8**, 3494–3511.
2. M. Kurakula, G. K. Rao and K. S. Yadav, in *Applications of advanced green materials*, Elsevier, 2021, pp. 395–423.
3. C. Shi, E. C. Quinn, W. T. Diment and E. Y.-X. Chen, *Chem. Rev.*, 2024, **124**, 4393–4478.
4. K. Min, J. D. Cuiffi and R. T. Mathers, *Nature Commun.*, 2020, **11**, 727.
5. J. Shen, W. Yuan, M. Badv, A. Moshaverinia and P. S. Weiss, *ACS Mater. Au*, 2023, **3**, 540–547.
6. M. D. Flamini, T. Lima, K. Corkum, N. J. Alvarez and V. Beachley, *Mater. Adv.*, 2022, **3**, 3303–3315.
7. D. Nath, M. Misra, F. Al-Daoud and A. K. Mohanty, *RSC Sustain.*, 2025, **3**, 1267–1302.

View Article Online
DOI: 10.1039/D5LP00403A

8. H. Liu, Y. Huang, L. Yuan, P. He, Z. Cai, Y. Shen, Y. Xu, Y. Yu and H. Xiong, *Carbohydr. Polym.*, 2010, **79**, 513–519.
9. P. Karimipour-Fard, M. P. Jeffrey, H. JonesTaggart, R. Pop-Iliev and G. Rizvi, *J. Mech. Behav. Biomed. Mater.*, 2021, **120**, 104583.
10. J. Yánez, V. Castillo, M. Matos, C. Rosales, M. Arnal and A. Müller, *E-polymer*, 2005.
11. A. Etale, A. J. Onyianta, S. R. Turner and S. J. Eichhorn, *Chem. Rev.*, 2023, **123**, 2016–2048.
12. M. Wahbi, Y. Wen, M. Kontopoulou and K. J. De France, *Carbohydr. Polym.*, 2025, **370**, 124471.
13. J. L. Fredricks, A. M. Jimenez, P. Grandgeorge, R. Meidl, E. Law, J. Fan and E. Roumeli, *J. Polym. Sci.*, 2023, **61**, 2585–2632.
14. J. Hou, B. E. Aydemir and A. G. Dumanli, *Philos. Trans. R. Soc. A*, 2021, **379**, 20200331.
15. M. Berroci, C. Vallejo and E. Lizundia, *ACS Sustain. Chem. Eng.*, 2022, **10**, 14280–14293.
16. H. Izadi, H. Asadi and M. Bemani, *Front. Mater.*, 2025, **12**, 1537067.
17. P. L. Chee, T. Sathasivam, Y. C. Tan, W. Wu, Y. Leow, Q. R. T. Lim, P. Y. M. Yew, Q. Zhu and D. Kai, *Nanoscale*, 2024, **16**, 3269–3292.
18. R. M. O'Dea, J. A. Willie and T. H. Epps, III, *ACS Macro Lett.*, 2020, **9**, 476–493.
19. A. J. Shapiro, apos, R. M. Dea, S. C. Li, J. C. Ajah, G. F. Bass and Epps, Thomas H., *Annu. Rev. Chem. Biomol. Eng.*, 2023, **14**, 109–140.
20. B. M. Sagar, M. M. Islam, M. L. Habib, S. Ahmed and M. S. Hossain, *RSC Adv.*, 2025, **15**, 26276–26301.
21. E. Lizundia, T.-D. Nguyen, R. J. Winnick and M. J. MacLachlan, *J. Mater. Chem. C*, 2021, **9**, 796–817.
22. W. M. Fazli Wan Nawawi, K.-Y. Lee, E. Kontturi, R. J. Murphy and A. Bismarck, *ACS Sustain. Chem. Eng.*, 2019, **7**, 6492–6496.
23. A. M. Salaberria, R. H. Diaz, M. A. Andrés, S. C. Fernandes and J. Labidi, *Materials*, 2017, **10**, 546.
24. A. Sanz de León, J. A. Pulido, N. Fernández-Delgado, F. J. Delgado and S. I. Molina, *ACS Appl. Mater. Interfaces*, 2024, **16**, 35554–35565.
25. M. K. Patel, F. Hansson, O. Pitkanen, S. Geng and K. Oksman, *ACS Appl. Polym. Mater.*, 2022, **4**, 6592–6601.
26. M. S. Irfan, R. Umer and S. Rao, *Fiber Polym.*, 2021, **22**, 1378–1387.
27. H. Yu, Z. Zhao, B. Xu, G.-H. Hu, C. Lemaitre and Y. Feng, *Industrial & Engineering Chemistry Research*, 2023, **62**, 17997–18008.
28. Z. Du, Y. Du, Y. Gong, G. Liu, Z. Li, G. Yu and S. Zhao, *RSC Adv.*, 2021, **11**, 35703–35710.
29. M. Azpitarte Aretxabaleta, G. Barandika, R. Minguez and E. Lizundia, *Biomacromolecules*, 2024, **25**, 7630–7641.
30. M. S. Alam, L. Sangroniz, M. Scoti, A. Gonzalez, A. Etxeberria, A. Sangroniz and E. Lizundia, *ACS Appl. Bio Mater.*, 2025, **8**, 10381–10392.
31. V. Sessini, B. Haseeb, A. Boldizar and G. L. Re, *RSC Adv.*, 2021, **11**, 637–656.
32. A. Lewandowski and K. Wilczyński, *Polymers*, 2022, **14**, 274.
33. N. Szpisják-Gulyás, A. N. Al-Tayawi, Z. H. Horváth, Z. László, S. Kertész and C. Hodúr, *Acta Aliment.*, 2023, **52**, 521–537.
34. L. Bai, L. Liu, M. Esquivel, B. L. Tardy, S. Huan, X. Niu, S. Liu, G. Yang, Y. Fan and O. J. Rojas, *Chem. Rev.*, 2022, **122**, 11604–11674.
35. M. Kaya, M. Mujtaba, H. Ehrlich, A. M. Salaberria, T. Baran, C. T. Amemiya, R. Galli, L. Akyuz, I. Sargin and J. Labidi, *Carbohydr. Polym.*, 2017, **176**, 177–186.

View Article Online
DOI: 10.1039/D5LP00403A

36. N. Yousefi, M. Jones, A. Bismarck and A. Mautner, *Carbohydr. Polym.*, 2021, **253**, 117273.
37. V. Grifoll, P. Bravo, M. N. Pérez, M. Perez-Clavijo, M. Garcia-Castrillo, A. Larrañaga and E. Lizundia, *ACS Sustain. Chem. Eng.*, 2024, **12**, 7869–7881.
38. A. Baxter, M. Dillon, K. A. Taylor and G. A. Roberts, *Int. J. Biol. Macromol.*, 1992, **14**, 166–169.
39. S. Duri and C. D. Tran, *Langmuir*, 2013, **29**, 5037–5049.
40. M. Thunwall, A. Boldizar and M. Rigdahl, *Biomacromolecules*, 2006, **7**, 981–986.
41. D. Rahardiyan, E. M. Moko, J. S. Tan and C. K. Lee, *Enzyme Microb. Technol.*, 2023, **168**, 110260.
42. A. Emblem, in *Packaging Technology*, eds. A. Emblem and H. Emblem, Woodhead Publishing, 2012, DOI: https://doi.org/10.1533/9780857095701.2.287, pp. 287–309.
43. J. Xu and B.-H. Guo, *Biotechnol. J.*, 2010, **5**, 1149–1163.
44. A. Ji, S. Bhagia, N. Han, K. H. Kim, G. Leem, N. C. Gallego, S. Zhang, K. Li, S. Ozcan, A. J. Ragauskas and C. G. Yoo, *RSC Sustain.*, 2025, **3**, 4478–4491.
45. A. Jabbarzadeh and B. Halfina, *Nanoscale Adv.*, 2019, **1**, 4704–4721.
46. M. Islam, A. S. K. Sinha and K. Prasad, *Sustainable Food Technol.*, 2026, DOI: 10.1039/D5FB00561B.
47. K. Schäler, A. Achilles, R. Bärenwald, C. Hackel and K. Saalwächter, *Macromolecules*, 2013, **46**, 7818–7825.
48. C. Baptista, A. Azagury, H. Shin, C. M. Baker, E. Ly, R. Lee and E. Mathiowitz, *Polymer*, 2020, **191**, 122227.
49. D. Ruiz, V. F. Michel, M. Niederberger and E. Lizundia, *Small*, 2023, **19**, 2303394.
50. T. M. Le, C. L. Tran, T. X. Nguyen, Y. H. P. Duong, P. K. Le and V. T. Tran, *J. Polym. Environ.*, 2023, **31**, 3094–3105.
51. C. Bouyahya, N. D. Bikiaris, A. Zamboulis, A. Kyritsis, M. Majdoub and P. A. Klonos, *Soft Matter*, 2022, **18**, 9216–9230.
52. D. H. U. Eranda, M. Chaijan and R. Castro-Munoz, *J. Food Eng.*, 2025, **391**, 112440.
53. D. Yu, X. Zhao, A. P. Amores, Y. Wang, J. Dutta, J.-L. Yang and F. Ye, *Int. J. Biol. Macromol.*, 2025, 144713.
54. A. Larrañaga and E. Lizundia, *Eur. Polym. J.*, 2019, **121**, 109296.
55. A. Sarno, K. Olafsen, S. Kubowicz, F. Karimov, S. T. L. Sait, L. Sørensen and A. M. Booth, *Environmental Science & Technology Letters*, 2021, **8**, 250–255.
56. J. R. Dias, A. Sousa, A. Augusto, P. J. Bártolo and P. L. Granja, *Polymers (Basel)*, 2022, **14**.
57. C. T. Roberts and M. A. Grunlan, *ACS Macro Lett.*, 2025, **14**, 1221–1240.
58. J. Zhao, Y. Wang and C. Liu, *Food Analyt. Methods*, 2022, **15**, 2840–2846.

View Article Online
DOI: 10.1039/D5LP00403A

Dr Joshua C. Worch
Assistant Professor
Department of Chemistry
Virginia Tech
1040 Drillfield Drive
Davidson Hall, 313A
Blacksburg, Virginia 24061

19th December 2025

Re Data availability statement

All data are available in the manuscript or the supplementary information.

Best regards,

Joshua C. Worch